PRAMANA
— journal of
physics

© Printed in India

Vol. 45, No. 6,
December 1995
pp. 545–560

Propagation of a wavepacket on a model fractal lattice

P K CHATTARAJ* and S NATH†
Department of Chemistry, Indian Institute of Technology, Kharagpur 721 302, India
†Present address: Department of Physical Chemistry, Indian Association for the Cultivation of Science, Calcutta 700 032, India
*Author for correspondence

MS received 23 January 1995; revised 22 June 1995

Abstract. Dynamics of a wavepacket on a model fractal surface has been studied by solving the pertinent time dependent Schrödinger equation. Spatial and temporal behaviour of charge and current densities and a local chemical potential for two different fractal lattices have been considered. Important insight into the dynamics has been obtained through time dependence of various quantities like macroscopic kinetic energy, global current, Shanon entropy, density correlation and global chemical potential. This study would be helpful in simulating adsorption and catalysis.

Keywords. Fractal surface; spatio temporal variations.

PACS Nos 05·45; 47·53; 34·10; 82·65

1. Introduction

One of the commonly used methods of studying dynamical problems is to follow the time evolution of a wavepacket through numerical integration of the pertinent time dependent Schrödinger equation (TDSE). Different variants of this method successfully accounted for various time dependent processes like chemical reactions [1, 2], collision induced dissociation [3, 4], gas-surface scattering [5], photodissociation [6], photoabsorption and emission [7], Raman scattering [8], atom diffraction by surfaces [9], etc. An excellent review [10] on this subject has also been published. In recent years wavepacket dynamics has been extensively used [11–16] in understanding quantum domain behaviour of a classically chaotic system. Since any chaotic system is geometrically characterized [17] by its scale invariance property a detailed knowledge of the corresponding fractal [18] behaviour is important. This study is supposed to provide [19–22] a connection between structural and dynamical information. As has been pointed out [23] the relevance of fractal behaviour is likely to be manifested in heterogeneous reaction dynamics which has been explicitly demonstrated [24] in a study of catalytic properties of solid surfaces. Another way is to simulate a catalyst or any disordered surface in general as a fractal surface, e.g. the diffusion-limited aggregate [25–27], devil's staircase [28] or a Cantor set [28] like structure. In this article we have solved the pertinent TDSE to study the dynamics of a wavepacket on a model fractal lattice. While methodology is discussed in § 2, a brief outline of the numerical solution is given in § 3. In § 4 the results and discussion are presented. Finally, § 5 contains some concluding remarks.

2. Methodology

The time dependent Schrödinger equation for a single particle moving under some external potential can be written as (in a.u.)

$$\left[-\frac{1}{2}\nabla^2 + v(r,t)\right]\psi(r,t) = i\frac{\partial\psi(r,t)}{\partial t}. \tag{1}$$

Dynamics of a single particle, simulated by a wavepacket, on a model fractal lattice can be studied by solving (1). The external potential $v(r,t)$ arising from a fractal lattice of embedding Euclidean dimension two has been formulated as,

$$v(x,y) = -\sum_i \sum_j \frac{1}{[(x-a_i)^2 + (y-b_j)^2]^{1/2}} \tag{2}$$

where (a_i, b_j) denote the Cartesian coordinates of a point on the fractal lattice which acts as an attractive Coulomb source of unit charge. The points $\{(a_i, b_j)\}$ are obtained as follows. Start with a conventional Cantor set-like fractal lattice of dimension log 2/log 3. Take the interval (0, 1), divide it into three equal segments and delete the central one (1/3, 2/3). The process is continued until the third generation lattice with 16 lattice points is obtained. A two-dimensional extension to this lattice has been generated by replacing each point of this horizontal Cantor lattice by a similar vertical Cantor lattice with an overall fractal dimension [18] 2log 2/log 3. Finally these points are normalized to have the lattice points. We term this lattice as lattice I. For comparison, another lattice of dimension 2log 3/log 5 has been constructed in its second generation with 18 lattice points. This lattice is termed as lattice II. It may be noted that external potential given in (5) does not contain any time. For a real system explicit time dependence may come from the relative motion between the target and the projectile and/or the oscillation of the lattice. Thus, the dynamics in the present study has only implicit time dependence arising from the temporal evolution of the wavepacket.

3. Numerical solution

The numerical solution is launched with the following initial and boundary conditions

$$\begin{aligned} \psi(x,y,0) &= \frac{1}{\sqrt{\pi}}\exp\left[-\frac{1}{2}(x^2+y^2)\right] \\ \psi(\pm\infty, y, t) &= 0 \quad \forall y, t \\ \psi(x, \pm\infty, t) &= 0 \quad \forall x, t. \end{aligned} \tag{3}$$

The TDSE (1) is solved using an alternating direction implicit (ADI) finite difference algorithm [29] with the above initial and boundary conditions. Spatial and temporal mesh sizes adopted here are $\Delta x = \Delta y = 0{\cdot}097$ and $\Delta t = 0{\cdot}01$. Spatial grid has been chosen in such a way that it avoids singularity associated with the Coulomb potential in (2). Each ADI cycle comprises two steps, i) substitute all x derivatives by Cranck-Nicolson analogues and y derivatives by explicit scheme. Therefore the finite difference

analogue (FDA) of (1) at a mesh point (x_l, y_m) becomes

$$c_l \psi_{l-1,m}^{n+1} + a_l \psi_{l,m}^{n+1} + b_l \psi_{l+1,m}^{n+1} = d_l \tag{4}$$

where,

$$c_l = b_l = \frac{i}{4(\Delta x)^2},$$

$$a_l = -\left(\frac{i}{2(\Delta x)^2} + \frac{i v_{l,m}}{2} + \frac{1}{\Delta t}\right)$$

and

$$d_l = \psi_{l,m}^{n}\left(\frac{i v_{l,m}}{2} - \frac{1}{\Delta t}\right) - \frac{i}{4}\frac{\partial^2 \psi}{\partial x^2} - \frac{i}{2}\frac{\partial^2 \psi}{\partial y^2}.$$

Explicit FDA of derivatives in d_l of (4) are used; (ii) in the next step Cranck-Nicolson explicit sequence is reversed and the corresponding FDA of (1) becomes

$$c_m \psi_{l,m-1}^{n+2} + a_m \psi_{l,m}^{n+2} + b_m \psi_{l,m+1}^{n+2} = d_m \tag{5}$$

where

$$c_m = b_m = \frac{i}{4(\Delta y)^2},$$

$$a_m = -\left(\frac{i}{2(\Delta y)^2} + \frac{i v_{l,m}}{2} + \frac{1}{\Delta t}\right)$$

and

$$d_m = \psi_{l,m}^{n+1}\left(\frac{i v_{l,m}}{2} - \frac{1}{\Delta t}\right) - \frac{i}{4}\frac{\partial^2 \psi}{\partial y^2} - \frac{i}{2}\frac{\partial^2 \psi}{\partial x^2}.$$

In order to follow the dynamics we have also calculated the following quantities:

a) charge density given by

$$\rho(r, t) = |\psi(r, t)|^2,$$

b) current density given by

$$j(r, t) = \psi_{re} \nabla \psi_{im} - \psi_{im} \nabla \psi_{re'},$$

c) global current defined as

$$j = \int |j(r, t)| \rho(r, t) \mathrm{d}r,$$

d) Shanon entropy as

$$S = -k \int \rho(r, t) \ln \rho(r, t) \mathrm{d}r,$$

k being the Boltzmann constant,

e) density correlation as

$$C = 2\pi \int \rho(r, 0)\, \rho(r, t) \mathrm{d}r,$$

f) macroscopic kinetic energy as

$$T = \frac{1}{2}\int \frac{|j|^2}{\rho}\,\mathrm{d}r$$

g) local chemical potential defined as [30]

$$\mu(r,t) = \frac{\delta E(t)}{\delta \rho} = \frac{1}{8}\left[\left(\frac{\nabla\rho}{\rho}\right)^2 - \frac{2\nabla^2\rho}{\rho}\right] + \frac{1}{2}\left(\frac{j}{\rho}\right)^2 + v$$

and

h) chemical potential as,

$$\mu(t) = \int \mu(r,t)\,\rho(r,t)\mathrm{d}r.$$

4. Results and discussion

Figures 1a and 1b depict the spatial behaviour of external potentials associated with two different fractal lattices (I and II). Local extrema in these plots are different both in magnitude and in position.

Time evolution of charge density profile is presented in figures 2a to 2e. Initial density profile (figure 2a) gets decomposed and dispersed in course of time over lattice I (figures 2b and 2c, at $t = 0{\cdot}16$ and 1 respectively) and lattice II (figures 2d and 2e, at $t = 0{\cdot}16$ and 1 respectively). Although the initial decomposition patterns (figures 2b and 2d) are different in two lattices, the long time behaviour (figures 2c and 2e) is similar but

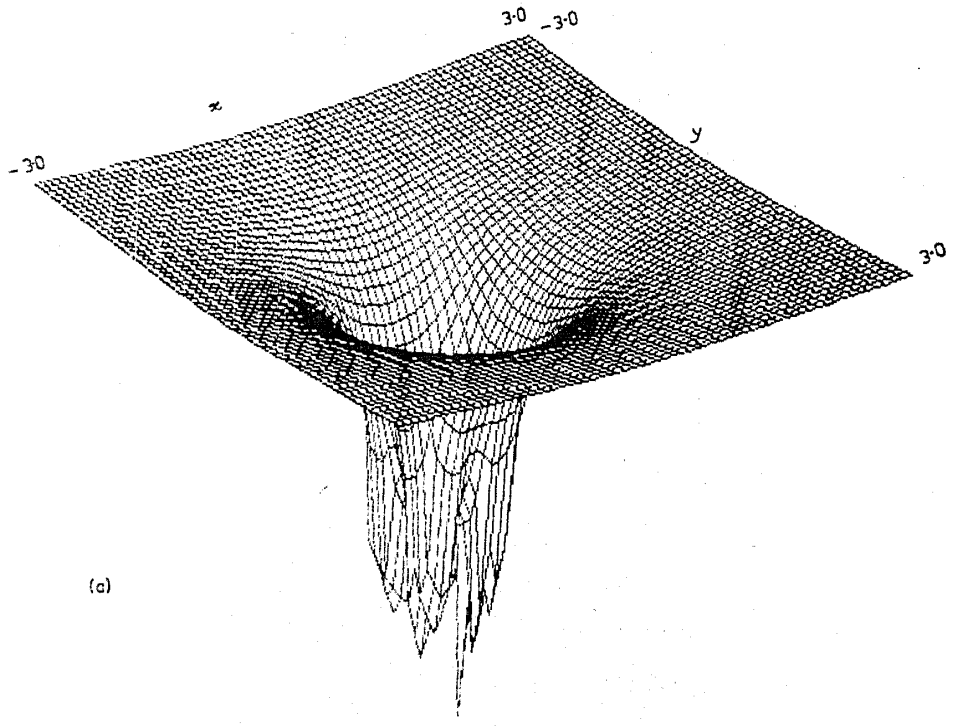

Figure 1a.

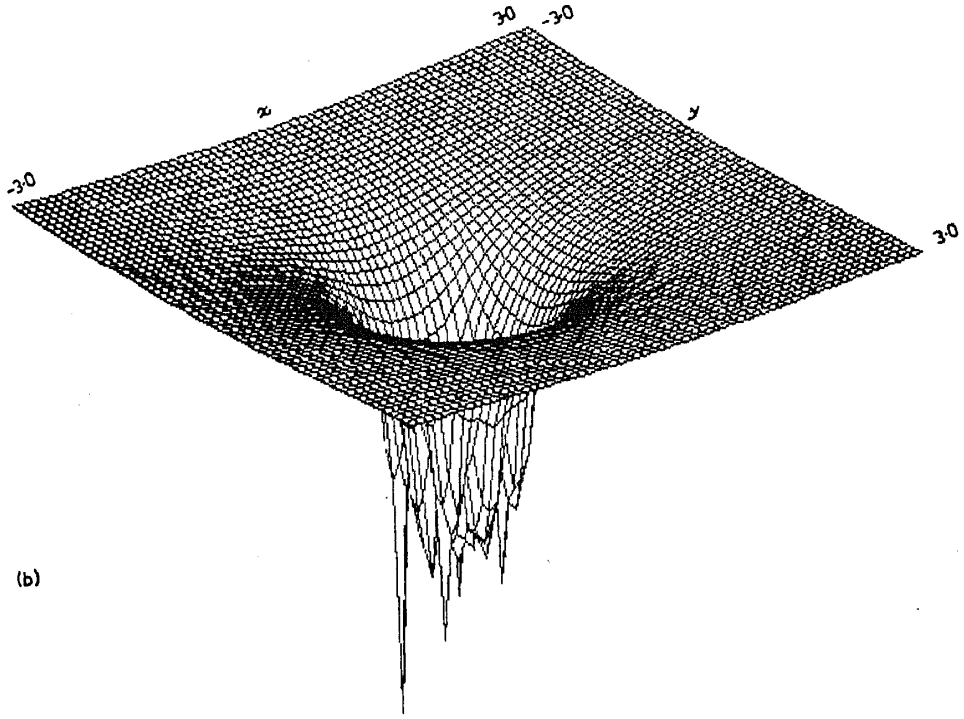

Figure 1. Spatial profile of external potential for propagation of a wavepacket on model fractal lattices. The basal square mesh designates $-3 \leqslant x \leqslant 3$ and $-3 \leqslant y \leqslant 3$ (**a**) Lattice I; (**b**) Lattice II.

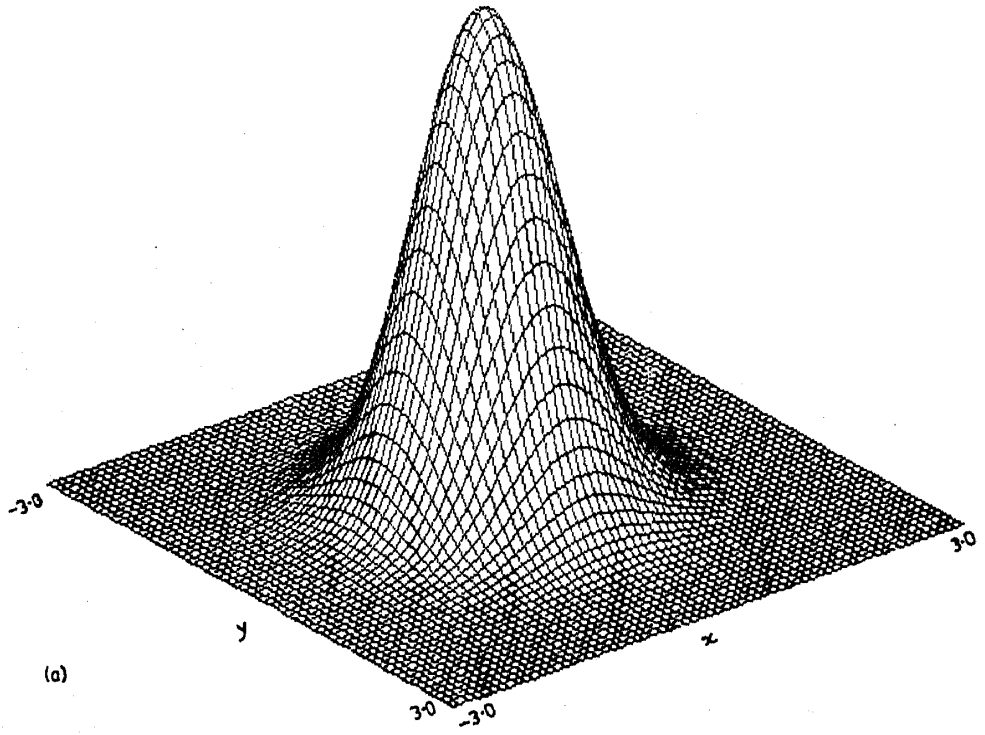

Figure 2a.

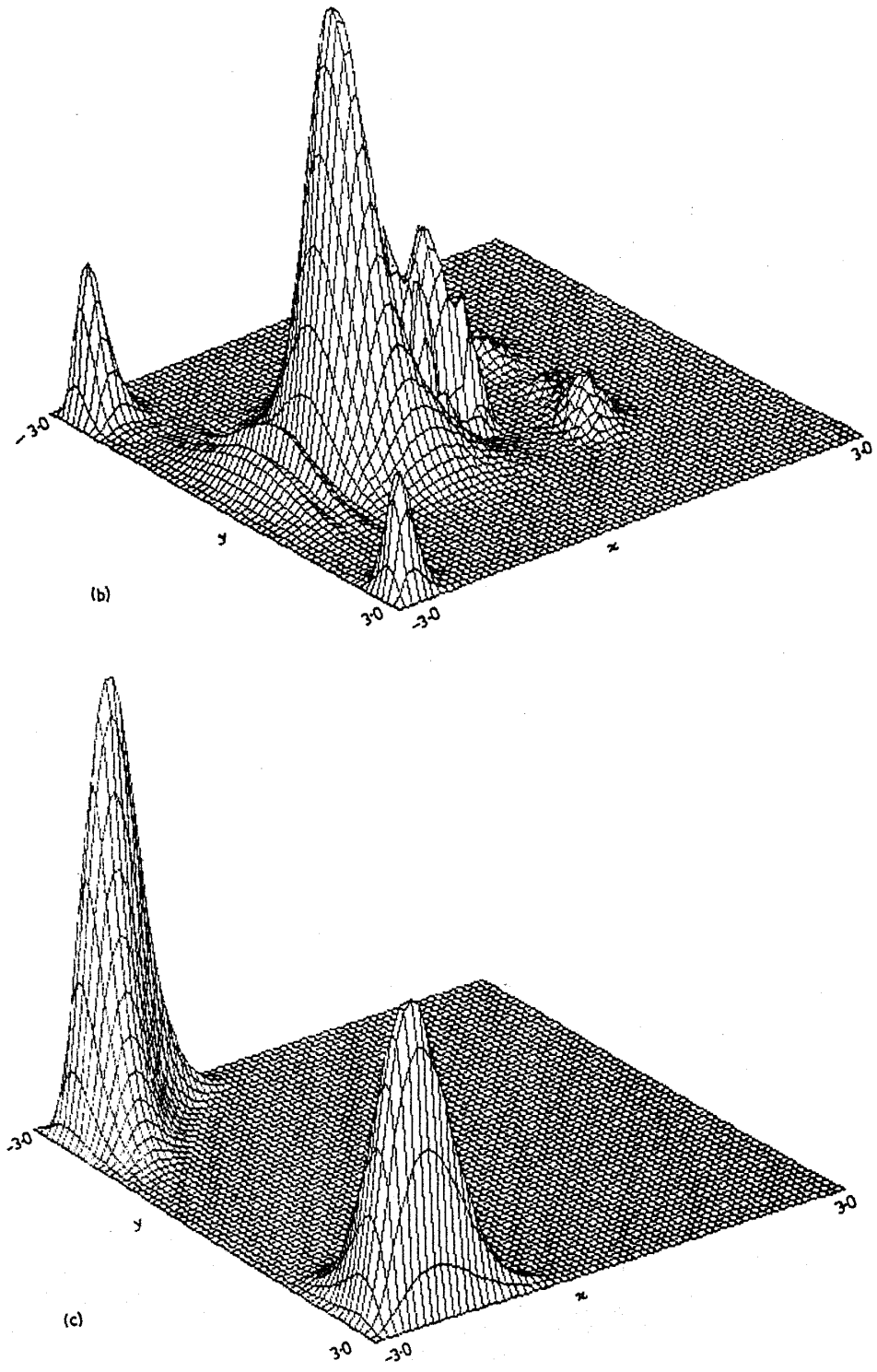

Figure 2b–c.

for different peak heights. While kinetic energy operator tries to move the wavepacket the attractive coulomb operator likes it to be localized in the fractal lattice points. Overall dynamics of the wavepacket is governed by an interplay of these kinetic and

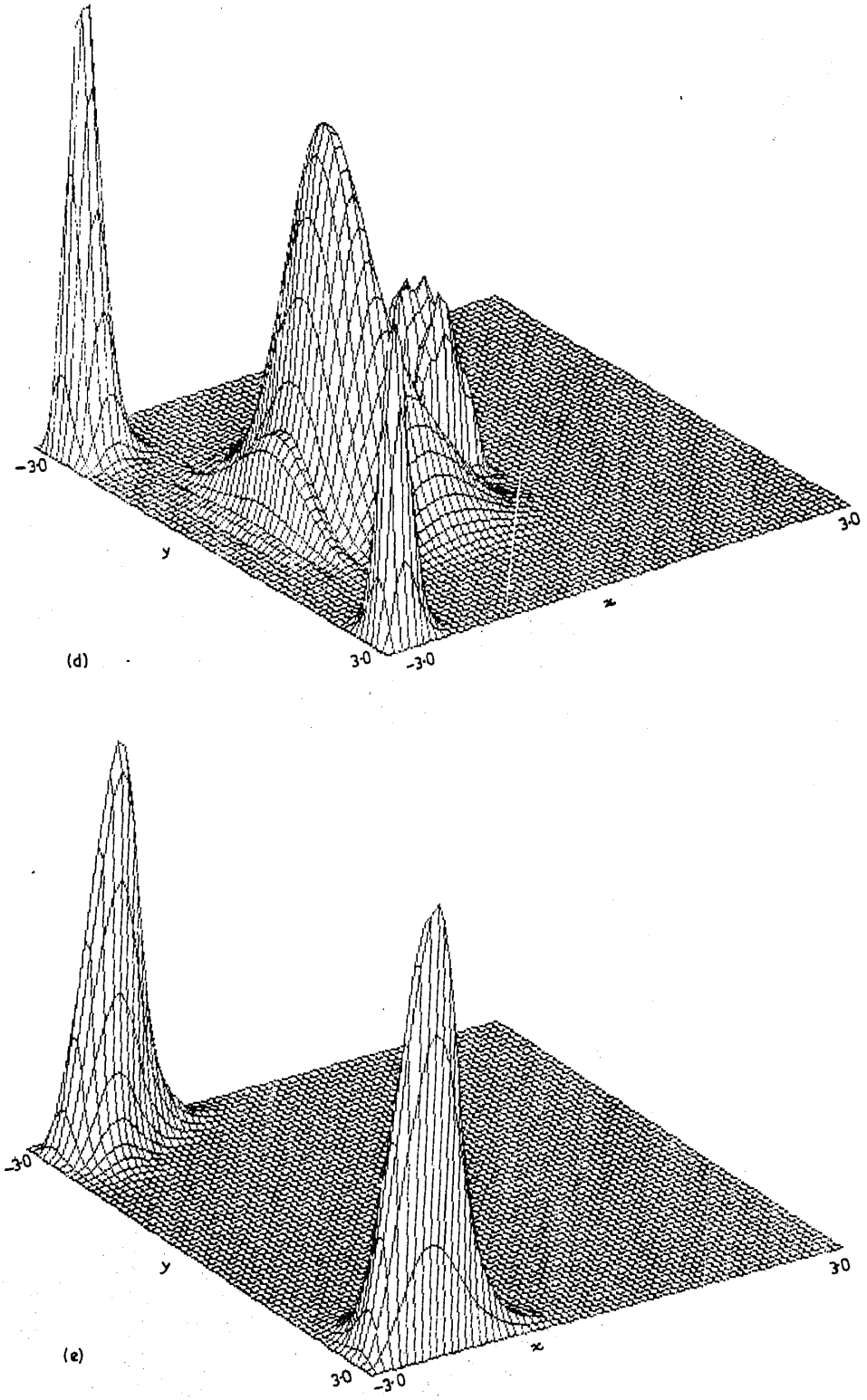

Figure 2. Spatial profile of density (**a**) $t = 0$; (**b**), (**c**) lattice I, $t = 0{\cdot}16$, 1 and (**d**), (**e**) lattice II, $t = 0{\cdot}16$, 1. See caption of figure 1 for details.

potential effects. Potential effect is dominant at the beginning and the wavepacket is mostly localized around coulomb attractors. As time progresses the kinetic effect takes over and the probability of getting the particle maximizes (albeit unequal) in two zones near the edges of the mesh and away from coulomb centres.

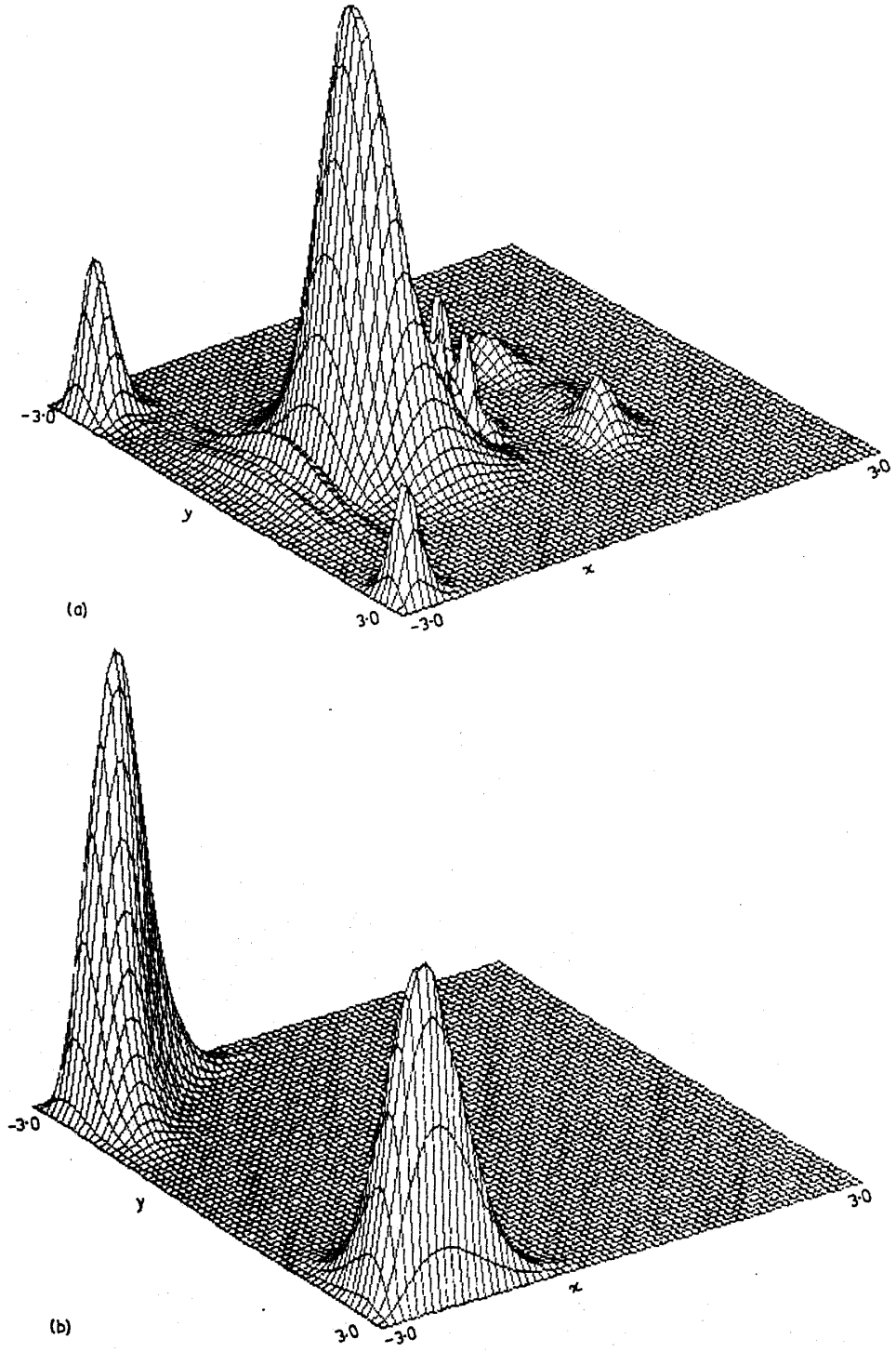

Figure 3a–b.

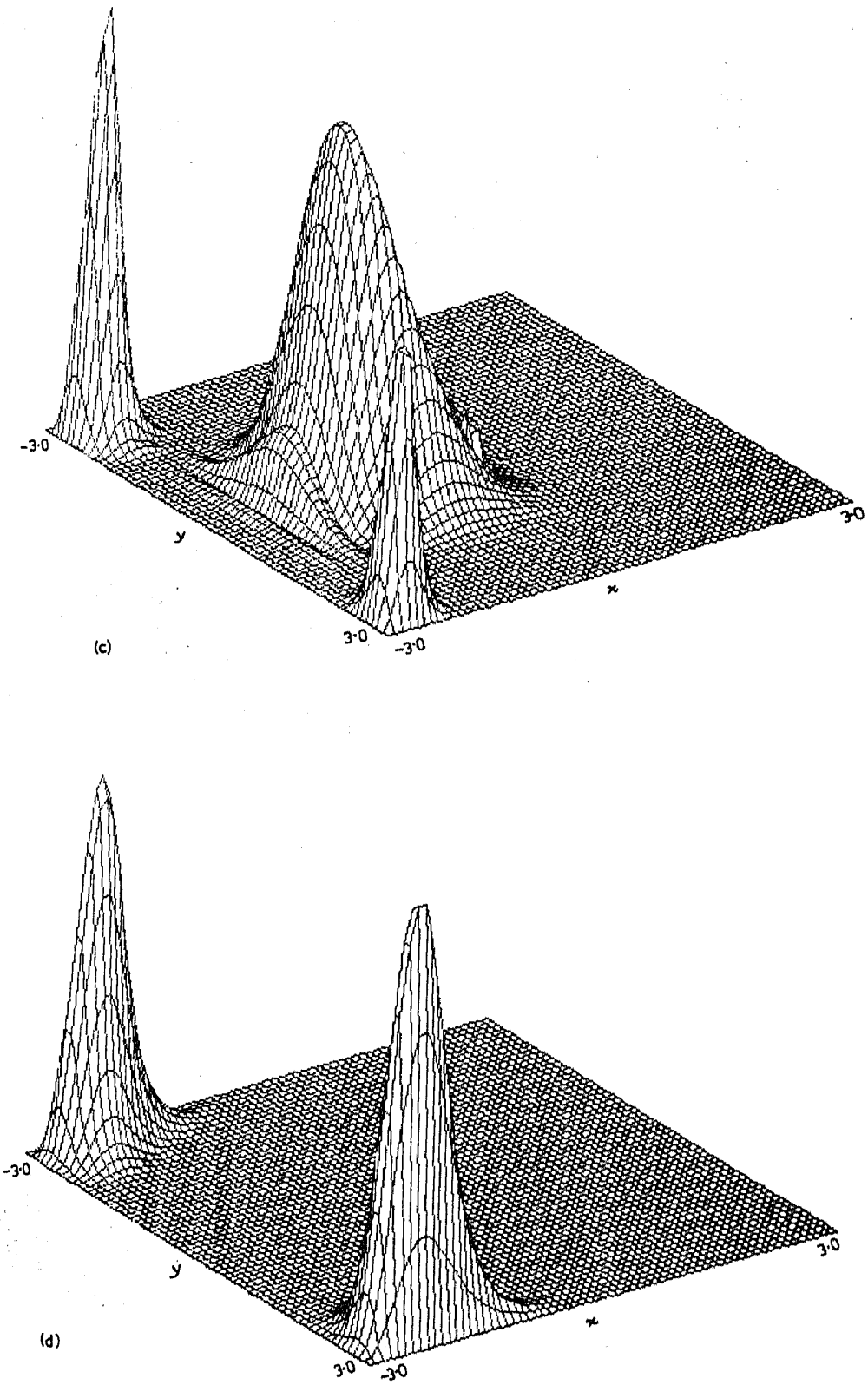

Figure 3. Spatial profile of current density (**a**), (**b**) lattice I, $t = 0{\cdot}16$, 1 and (**c**), (**d**) lattice II, $t = 0{\cdot}16$, 1. See caption of figure 1 for details.

Figures 3a to 3d show the temporal evolution of current density. Starting from an initial zero value it starts accumulating at different positions of the lattice commensurate with the local accumulation and depletion in density distribution (figure 2). Like in density plots, the short-time behaviour of j is markedly different in two lattices and the difference is reduced as time progresses. Out of the two accessible zones the probability of getting the particle is more where the current density is higher.

The most intricate dynamical behaviour is revealed through the plots of local chemical potential (figures 4a to 4e). It starts from a cot-like structure at $t = 0$. Since in

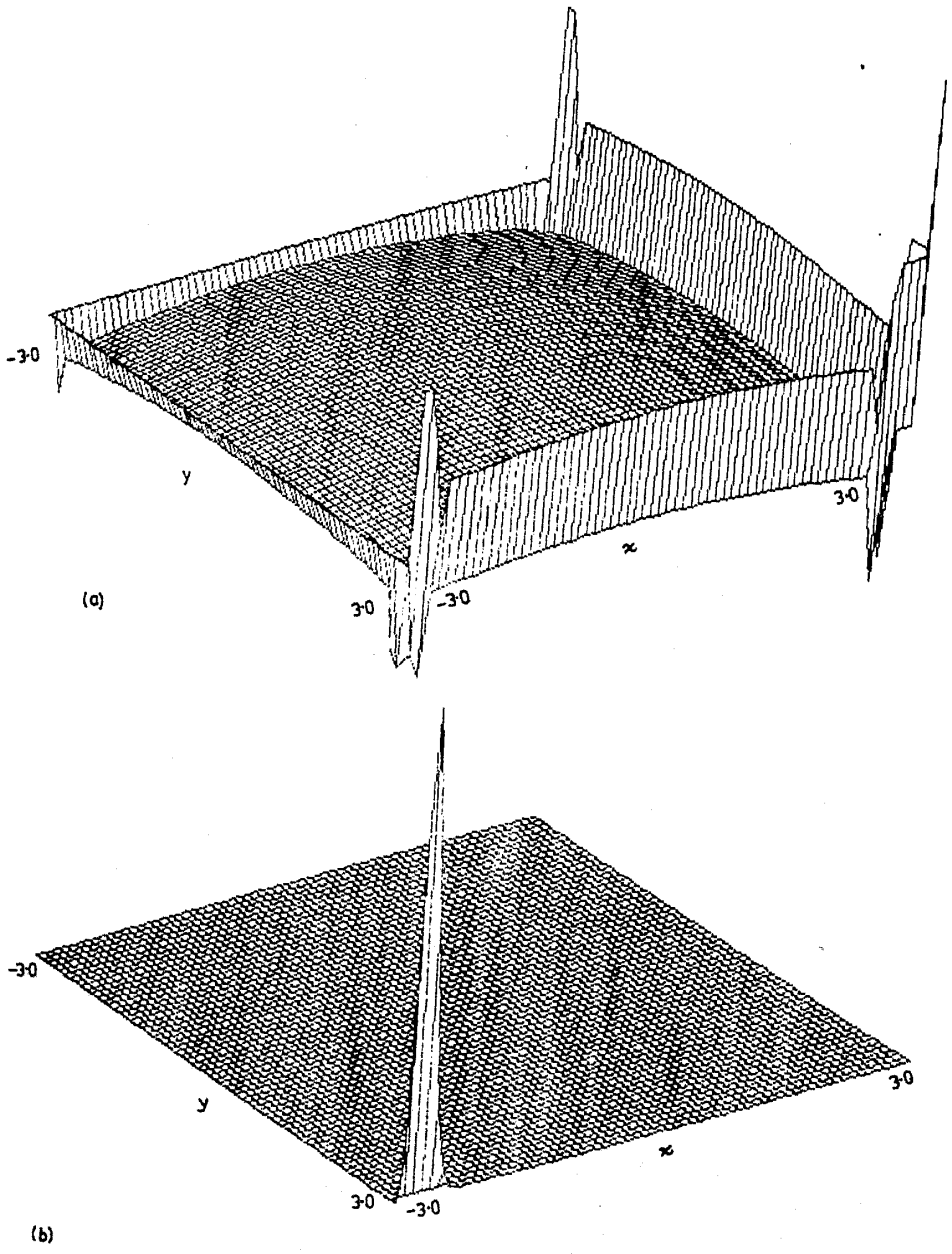

Figure 4a–b.

the present problem v does not vary with time local chemical potential is plotted relative to v in figure 3. Local chemical potential gets concentrated at a specific site and its base broadens in course of time. This site is around one of the two zones discussed above. High positive values of μ here reveal that energy of the system increases on charge accumulation and hence the lower current/probability zone does not like further charge transfer towards it.

Figures 5–9 depict respectively the time variations of global current, Shanon entropy, density correlation, macroscopic kinetic energy and chemical potential. In each figure two different curves refer to lattices I and II respectively. As expected, although the numerical values differ the overall behaviour of a given quantity remains same in two lattices in all figures. Global current increases to a maximum value around

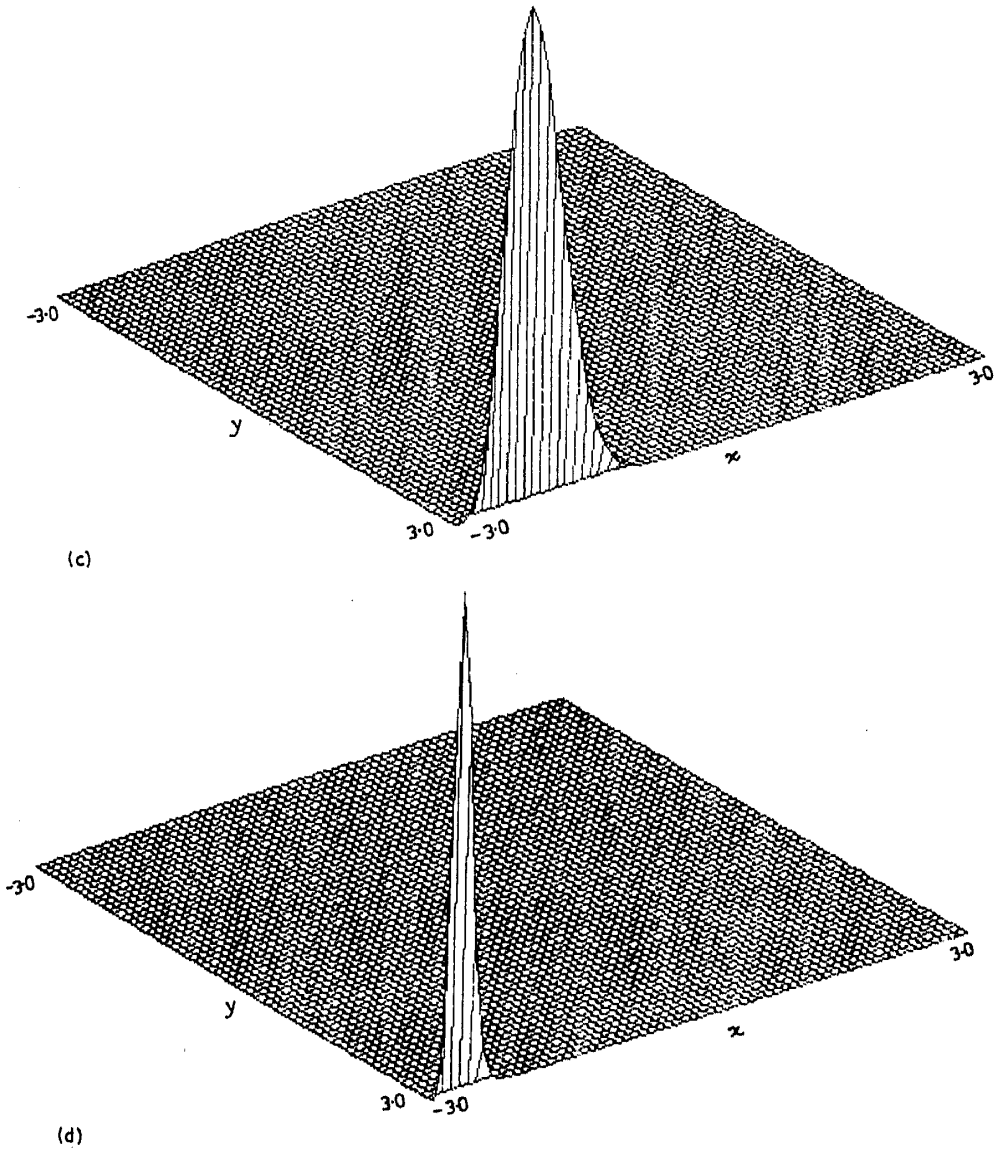

Figure 4c–d.

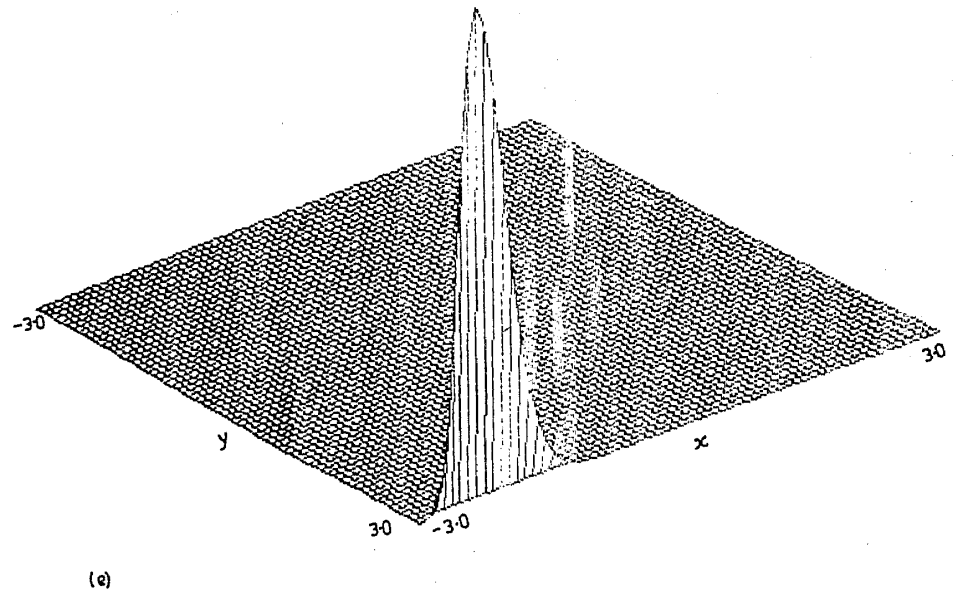

(e)

Figure 4. Spatial profile of local chemical potential (**a**) $t = 0$; (**b**), (**c**) lattice I, $t = 0{\cdot}16$, 1 and (**d**), (**e**) lattice II, $t = 0{\cdot}16$, 1. See caption of figure 1 for details.

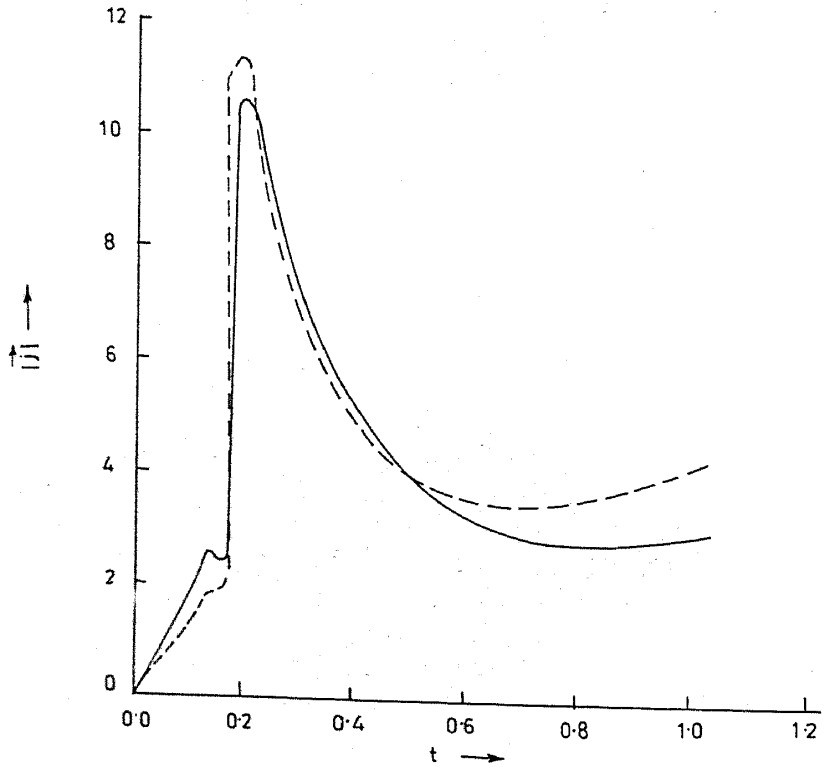

Figure 5. Temporal evolution of global current (a) (———) lattice I, (b) (– – –) lattice II. See caption of figure 1 for details.

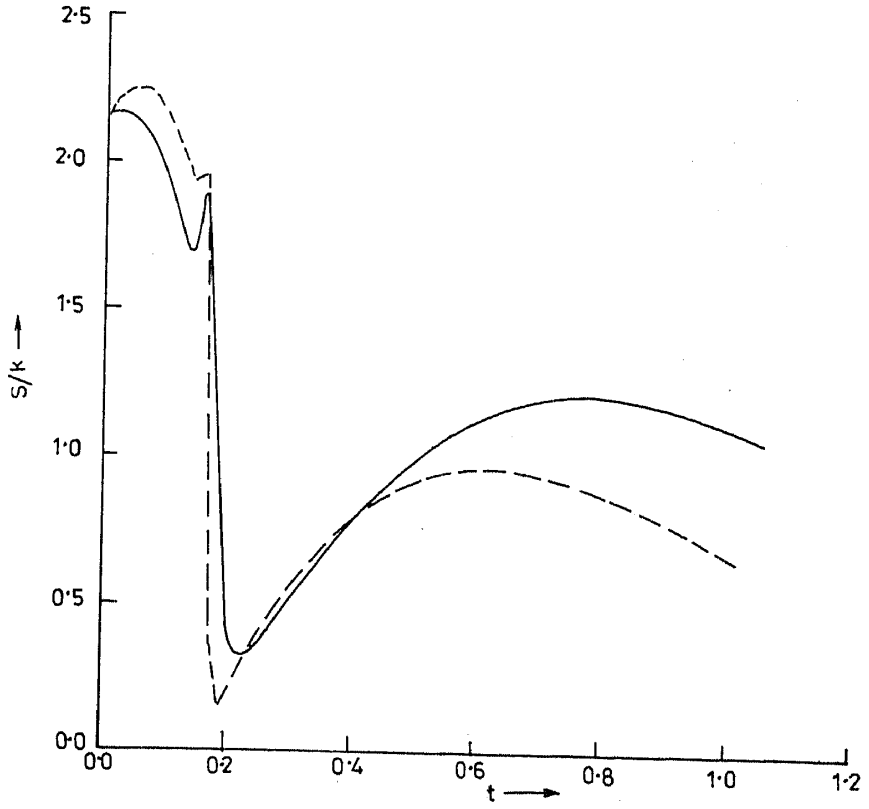

Figure 6. Temporal evolution of Shanon entropy (a) (———) lattice I, (b) (– – –) lattice II. See caption of figure 1 for details.

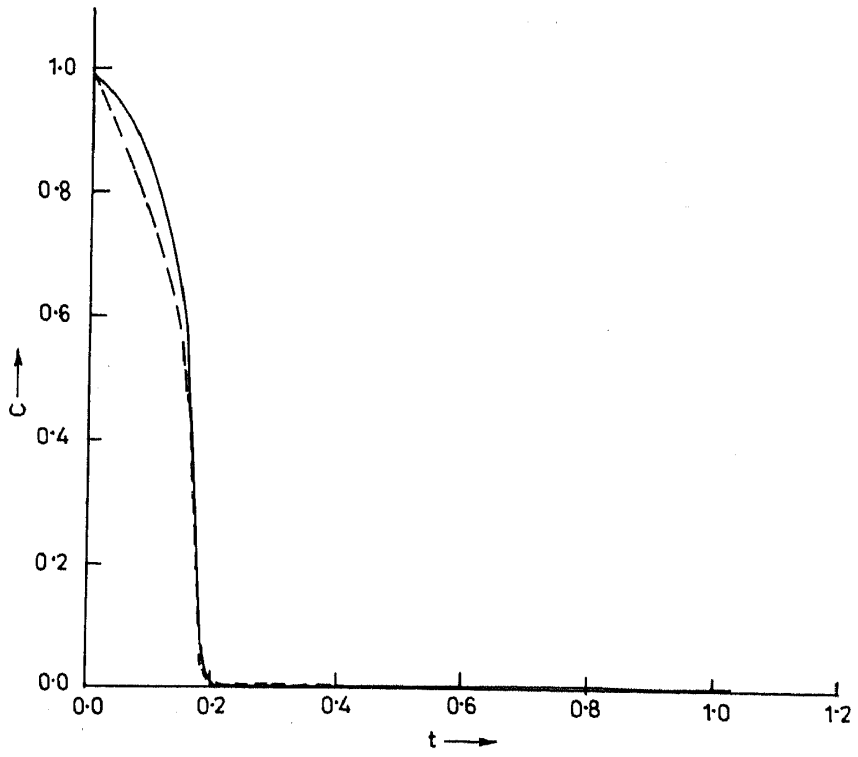

Figure 7. Temporal evolution of density correlation (a) (———) lattice I, (b) (– – –) lattice II. See caption of figure 1 for details.

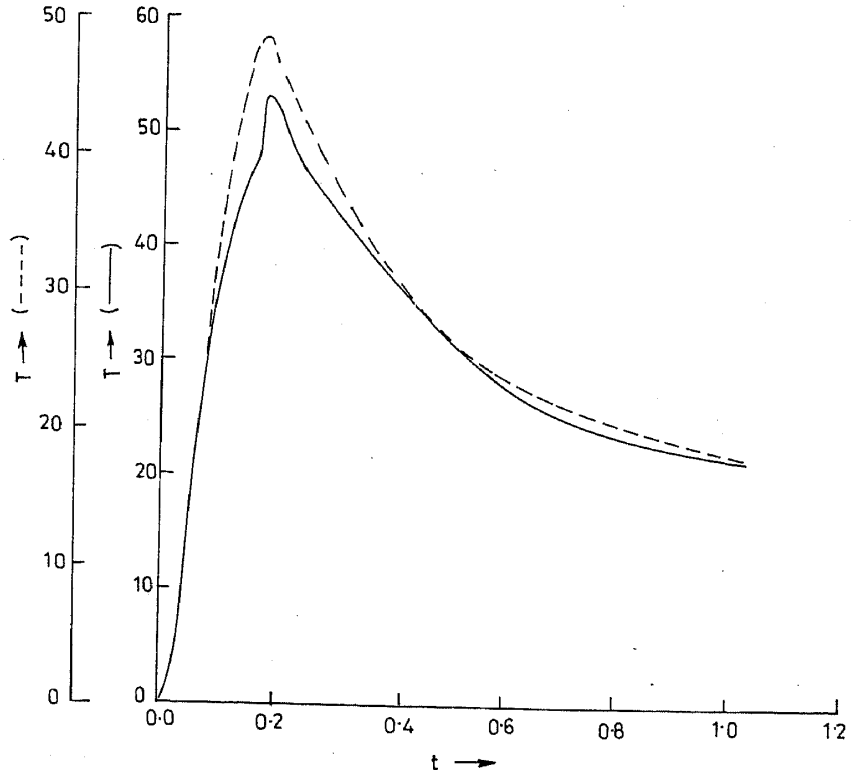

Figure 8. Temporal evolution of macroscopic kinetic energy (a) (———) lattice I, (b) (– – –) lattice II. See caption of figure 1 for details.

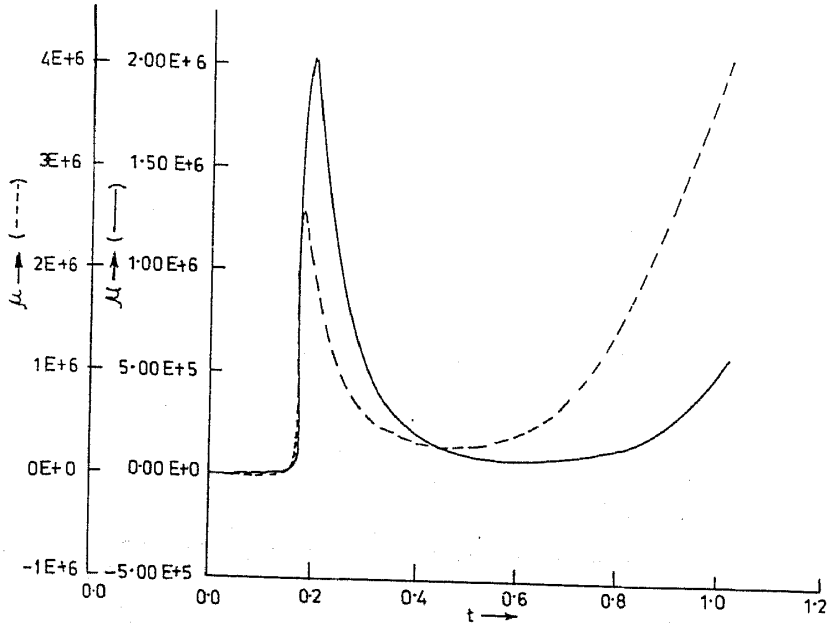

Figure 9. Temporal evolution of chemical potential (a) (———) lattice I, (b) (– – –) lattice II. See caption of figure 1 for details.

$t = 0{\cdot}2$ where kinetic energy also becomes maximum. Density correlation starts decreasing from an initial value unity. At around $t = 0{\cdot}2$ it goes to zero and system loses its correlation with its initial state. At $t = 0$, Shanon entropy has the value $k(1 + \ln \pi)$, k being the Boltzmann constant. It starts oscillating with time and a local maximum in entropy (a measure of disorderliness) slightly before $t = 0{\cdot}2$ goes along with maxima in global current and KE and zero value of correlation. However, the minimum in entropy around $t = 0{\cdot}2$ is apparently not in conformity with extremal behaviour of other quantities at that time step. Entropy then starts increasing and a broad maximum in it, zero value of correlation and very small values for current and KE are internally consistent. Global chemical potential starts from a negative value ($-360{\cdot}28$ and $-466{\cdot}43$ for lattices I and II respectively at $t = 0$ which are not conspicuous in the figures) and increases rapidly to a maximum positive value around $t = 0{\cdot}2$. Then it starts decreasing and passes through a broad minimum. Since its extremal characteristic as a function of time resembles that of current density it can be treated as a useful index for studying dynamical problems. This quantity contains information of the correct time of charge transfer such that the change in the energy of the system stabilizes it the most.

5. Concluding remarks

Important insight into the dynamics of a wavepacket on a model fractal lattice has been obtained through spatial and temporal variations of several quantities which depend on time dependent charge and current densities. Interplay of kinetic and potential effects governs the overall dynamics. Initially the wavepacket remains confined around coulomb centres of the fractal lattice. In course of time there result two accessible zones around the edges, away from the coulomb sources. Local chemical potential exhibits intriguing spatio-temporal behaviour. Different time dependent quantities extremize in time in a consistent manner. After certain time most of these quantities do not change appreciably. Chemical potential seems to contain valuable dynamical information and deserves closer scrutiny. As expected the qualitative behaviour of various dynamical quantities in two lattices is similar although they differ quantitatively. At this stage the exact connection between structure of the surface and the resulting dynamical information is not clear. However, the dependence of the dynamical observables on the fractal behaviour of the lattice is conspicuous.

Acknowledgement

The authors would like to thank the referee for constructive criticism and one of them (SN) would like to thank CSIR, New Delhi for financial assistance.

References

[1] J Mazur and R J Rubin, *J. Chem. Phys.* **31**, 1395 (1959)
[2] E A McCullough Jr and R E Wyatt, *J. Chem. Phys.* **51**, 1253 (1969)
[3] K C Kulander, *J. Chem. Phys.* **69**, 5064 (1978)
[4] C Leforestier, *Chem. Phys.* **87**, 241 (1984)

[5] R B Gerber, R Kosloff and M Berman, *Comput. Phys. Rep.* **5**, 59 (1986)
[6] E J Heller, *J. Chem. Phys.* **68**, 2066 (1978)
[7] E J Heller, *Acc. Chem. Res.* **14**, 368 (1981)
[8] D J Tannor and E J Heller, *J. Chem. Phys.* **77**, 202 (1982)
[9] G Drolshagen and E J Heller, *J. Chem. Phys.* **79**, 2072 (1983)
[10] V Mohan and N Sathyamurthy, *Comput. Phys. Rep.* **7**, 213 (1988)
[11] P Brumer and M Shapiro, *Chem. Phys. Lett.* **72**, 528 (1980)
[12] M J Davis, E B Stechel and E J Heller, *Chem. Phys. Lett.* **76**, 21 (1980)
[13] J S Hutchinson and R E Wyatt, *Phys. Rev.* **A23**, 1567 (1981)
[14] M Bixon and J Jortner, *J. Chem. Phys.* **77**, 4175 (1982)
[15] M D Feit and J A Fleck Jr, *J. Chem. Phys.* **80**, 2578 (1984)
[16] P K Chattaraj and S Sengupta, *Phys. Lett.* **A181**, 225 (1993)
P K Chattaraj, *Indian J. Pure Appl. Phys.* **32**, 101 (1994)
[17] Hao Bai-Lin, *Chaos* (Singapore: World Scientific, 1984)
[18] B B Mandelbrot, *The fractal geometry of nature* (New York: Freeman, 1982)
[19] H Singh and P K Chattaraj, *Proc. Indian Acad. Sci. (Chem. Sci.)* **99**, 47 (1987)
[20] H Singh and P K Chattaraj, *Phys. Lett.* **A128**, 355 (1988)
[21] P K Chattaraj, *Chem. Phys. Lett.* **175**, 613 (1990)
[22] P K Chattaraj, *Symmetries and singularity structures: Integrability and chaos in nonlinear dynamical systems*, edited by M Lakshmanan and M Daniel (Berlin: Springer, 1990) pp 172–182
[23] P Pfeifer and D Avnir, *J. Chem. Phys.* **79**, 3558 (1983)
[24] P Meakin, *Chem. Phys. Lett.* **123**, 428 (1986)
[25] T A Witten Jr and L M Sander, *Phys. Chem. Rev.* **47**, 1400 (1981)
[26] T A Witten Jr and L M Sander, *Phys. Rev.* **B27**, 5686 (1983)
[27] S S Tambe, P Badola and B D Kulkarni, *Chem. Phys. Lett.* **173**, 67 (1990)
[28] R Gutfraind, M Sheintuch and D Avnir, *Chem. Phys. Lett.* **174**, 8 (1990)
[29] W F Ames, *Numerical methods for partial differential equations* (Academic: New York, 1977)
[30] P K Chattaraj and S Nath, *Int. J. Quantum Chem.* **49**, 705 (1994)
S Nath and P K Chattaraj, *Pramana – J. Phys.* **45**, 65 (1995)